CHAPTER IV

ETHYLENE EPOXIDATION OVER ALUMINA- AND SILICA-SUPPORTED SILVER CATALYSTS IN LOW-TEMPERATURE AC DIELECTRIC BARRIER DISCHARG

4.1 Abstract

In this work, ethylene epoxidation reaction for ethylene oxide production over silver catalysts loaded on two different supports (silica and alumina particles) in a low-temperature AC dielectric barrier discharge (DBD) reactor was investigated. The DBD plasma system was operated under the following base conditions: an O_2/C_2H_4 feed molar ratio of 1/4, a total feed flow rate of 50 cm^3/min, an electrode gap distance of 0.7 cm, an input frequency of 500 Hz, and an applied voltage of 19 kV. From the results, the presence of silver catalysts improved the ethylene oxide production performance. The silica support interestingly provided a higher ethylene oxide selectivity than the alumina support. The optimum Ag loading on the silica support was found to be 20 wt.%, exhibiting the highest ethylene oxide selectivity of 30.56%.

Keywords: Epoxidation; Ethylene oxide; Dielectric barrier discharge; Alumina; Silica; Silver

4.2 Introduction

As discovered by Lefort [1], ethylene oxide (C_2H_4O, EO) can be produced by partial oxidation of ethylene, so-called ethylene epoxidation. Recently, this reaction has been increasingly important for the petrochemical industry because EO is used as a feedstock for production of several chemicals. Most is currently converted to ethylene glycol, which is used to produce polyesters and also used as an antifreeze and automotive coolant. In addition, it is an important precursor to

produce surfactants by ethoxylation processes [2], and it is also employed as a sterilant for foodstuffs, in medical equipment and supplies, and as a fumigant in agricultural products [3].

Because of its various applications, many research studies have attempted to improve efficiency of ethylene epoxidation. Silver catalysts are generally used in this reaction, especially low-surface-area (LSA) α-alumina-supported silver catalyst (Ag/(LSA) α-Al$_2$O$_3$). Several second metals, such as Cs, Cu, Au and Re, loaded on silver catalysts, as well as chlorides added to reactant gases, have been proved to enhance EO selectivity [4-15]. In addition, the epoxidation activity is always affected by the properties of the supports [12,16-18]. Apart from the (LSA) α-Al$_2$O$_3$ support, SiO$_2$ support has been shown to provide high epoxidation activity [16,19,20]. These two supports are normally used in the ethylene epoxidation since they are not active in the further conversion of EO produced to acetaldehyde [19]. In addition, the SiO$_2$ support has been proved to possess some good properties as it is resistant to sintering and provides high metal dispersion compared to other supports [16]. Although the catalytic processes exhibit high EO selectivity, they still have some limitations, such as the requirement of high operating temperatures, leading to high energy consumption, and the deactivation of catalysts at high operating temperatures, e.g. coke formation and sintering of active sites on the catalyst surface, leading to decreases in catalytic activity and desired product selectivity. Therefore, new techniques and further catalyst development are required to solve these limitations and to increase efficiency of the epoxidation process.

Non-thermal plasma is a promising technique to be applied for several chemical reactions because the bulk gas temperature is comparatively low (maybe at room temperature or slightly higher) whereas the temperature of highly energetic electrons generated in plasma is very high [21,22]. These imply that the non-thermal plasma operated under atmospheric pressure and ambient temperature can result in low energy consumption. Moreover, it can overcome the above mentioned catalyst problems at high-temperature operation.

Due to their individual advantages of catalytic and plasma processes, there have been some research studies have attempted to combine a catalyst with a plasma system for improving the activity of chemical reactions [14,15,23]. In our previous

works [14,15,24], both the corona discharge and dielectric barrier discharge (DBD) were used to investigate the ethylene epoxidation reaction with and without silver catalysts. These results showed that a suitable silver catalyst combined with a plasma system provided a higher ethylene epoxidation activity as compared to the sole plasma system. In comparison, the DBD system provided better epoxidation performances in terms of C_2H_4 conversion, EO yield, and power consumption per EO molecule produced, as compared to the sole corona discharge system and the combined catalytic-corona discharge system. As described above, the DBD system has been found to have high potential performance for ethylene epoxidation, and the silver catalysts have been proved to enhance the epoxidation activity. Thus, it is interesting to apply silver catalysts in the DBD system for improving the ethylene epoxidation activity.

The main objective of this work was, for the first time, to investigate the combination of silver catalysts loaded on two different supports (SiO_2 and Al_2O_3 particles) in a low-temperature DBD system for ethylene epoxidation reaction. The effects of plasma volume-to-catalyst weight ratio, catalyst support, and silver loading on the epoxidation reaction efficiency in the terms of reactant conversion, EO yield, EO selectivity, and power consumption were examined in this work.

4.3 Experimental

4.3.1 Materials and Gases

Silver nitrate ($AgNO_3$), with 99.9% purity, supplied by Merck was used as the precursor for Ag catalysts. Alumina particles (Al_2O_3), supplied by PTT Co., Ltd., and silica particles (SiO_2), supplied by Merck, were used as the catalyst supports. The Al_2O_3 and SiO_2 particles had average diameters of 3–4 mm and 2 mm, respectively. All chemicals were used as received without further purification. The 99.995% helium (high purity grade), 40% ethylene balanced with helium, 97% oxygen balanced with helium, and 30% ethylene oxide balanced with helium used in this work were supplied by Thai Industrial Gas Co., Ltd.

4.3.2 Catalyst Preparation Procedures

The incipient wetness impregnation was used to prepare all supported Ag catalysts. The Al_2O_3 or SiO_2 particles were impregnated with an aqueous $AgNO_3$ solution to achieve various Ag loadings of 5 wt.%, 10 wt.%, 15 wt.%, and 20 wt.%. The mixture was then dried in air at 110 °C overnight. Finally, the desired prepared catalyst samples were calcined at 500 °C for 5 h [18]. For preparing the Ag loading over 20 wt.%, after the 20 wt.% Ag/SiO_2 was dried in air at 110 °C for 2 h, this catalyst was impregnated again with an aqueous $AgNO_3$ solution to achieve 25 wt.% and 30 wt.% Ag loadings.

4.3.3 Catalyst Characterization Techniques

The specific surface areas of all the prepared catalysts were determined by using a BET surface area analyzer (Quantachrome, Autosorb I) via nitrogen adsorption analysis at the liquid nitrogen temperature of -196 °C. The catalyst sample was outgassed under vacuum at 150 °C for 10 h prior to the analysis. The XRD patterns of all catalysts were obtained by using a Rigaku RINT 200 diffractometer equipped with a Ni-filtered $CuK\alpha$ radiation source and operated at 2θ ranging from 25° to 70° with a scaning rate of 5 °/min. A field emission scanning electron microscope (FE-SEM) equipped with an energy dispersive X-ray (EDX) analyzer was employed to investigate the surface morphology of a catalyst sample and to evaluate the approximate particle size distribution. The catalyst sample was coated with platinum prior to loading into the microscope. Temperature-programmed oxidation (TPO) was employed to determine the amount of coke formation on the surface of spent catalysts. The oxygen balanced with helium at a molar ratio of 2/1 and a total flow rate of 40 cm^3/min was flown through the sample. The sample temperature was linearly increased from room temperature to 850 °C with a constant rate of 10 °C/min to ensure that the carbon (coke) deposit on the spent catalyst surface was completely oxidized to CO_2. The effluent CO_2 was then converted to CH_4 by a methanator containing Ni/Al_2O_3 catalyst at 400 °C. Finally, a flame ionization detector (FID, SRI model 110) was employed to detect the produced CH_4, which was used to subsequently calculate the amount of coke formed on the spent catalyst surface.

### 4.3.4 Catalytic Activity Experiments

The ethylene epoxidation reaction was investigated over the prepared silver catalysts in a parallel-plate dielectric barrier discharge (DBD) reactor at ambient temperature (25–27 °C) and atmospheric pressure. The schematic of the experimental setup is shown in Figure 4.1(a). The reactor was made of the acrylic plate with a 1.5 cm height, 5.5 cm width, and 17.5 cm length for the inner dimensions, and a 3.9 cm height, 9.5 cm width, and 21.5 cm length for the outer dimensions. It consisted of two parallel stainless steel electrodes and a dielectric glass plate placed on the lower electrode. The gap between two electrodes was fixed at 7 mm. The silver catalyst loaded on each of the two studied supports was placed in the gap, on the glass plate, and at the end region of the DBD reactor, as shown in Figure 4.1(b). An alternating current power (200 V and 50 Hz) was used as the input power to produce the microdischarge plasma in the electrode gap. The power supply unit consisted of three steps to convert an AC current power to a high voltage current. For the first step, the AC input power of 220 V and 50 Hz was transformed to the DC output of 70 Hz. Then, the DC output was converted to the AC current with a sinusoidal waveform and different frequencies by a 500 W power amplifier with a function generator. The outlet voltage was subsequently stepped up by using a high voltage transformer. Finally, the high voltage AC current was produced, and its output voltage and frequency were adjusted by the function generator, whereas its sinusoidal wave signal was monitored by an oscilloscope. The description of the power supply unit was given elsewhere [25]. Because the generated microdischarge plasma was found to be non-equilibrium in nature, the high-side voltage and current were not able to be directly measured across the electrodes. Hence, the voltage and current were measured accurately at the low voltage side instead, whereas the high-side voltage and current were calculated by multiplying and dividing by a factor of 130, respectively. The power, frequency, and voltage were measured by a power analyzer at the low voltage side of the power supply unit.

(a)
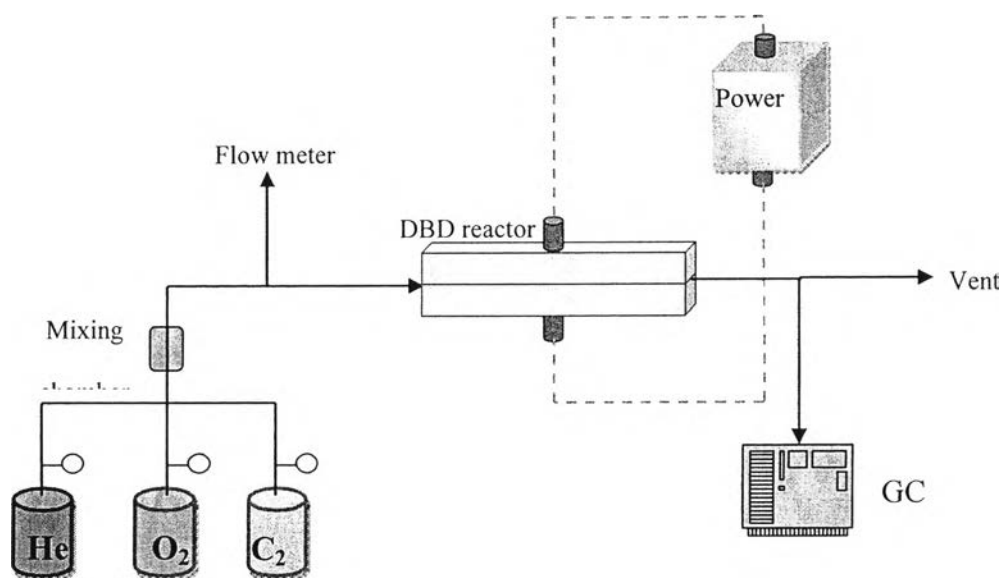
(b)
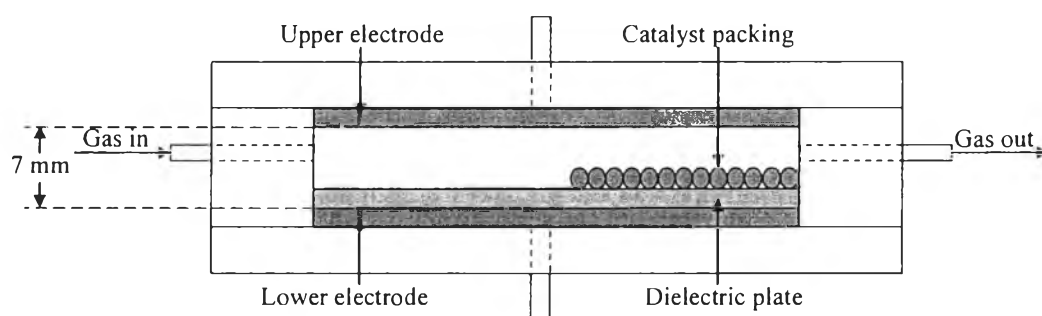
Figure 4.1 (a) Schematic of experimental setup of DBD plasma system for ethylene epoxidation reaction and (b) the configuration of the DBD reactor.

For reaction testing experiments, reactant gases of ethylene, oxygen, and helium were fed into the DBD plasma system and were controlled by electronic mass flow controllers. The studied DBD plasma system was operated under the base

conditions described in our previous work [26], which were an O_2/C_2H_4 feed molar ratio of 1/4, a total feed flow rate of 50 cm^3/min, an electrode gap distance of 0.7 cm, an input frequency of 500 Hz, and an applied voltage of 19 kV. The effects of Ag loading and support on the ethylene epoxidation reaction were investigated in this work. The product gas was allowed to pass through a water trap filter before being fed to an on-line gas chromatograph. After the studied DBD system reached steady state, the compositions of feed and product gases were analyzed by an on-line gas chromatograph (PerkinElmer, AutoSystem GC) equipped with both a thermal conductivity detector (TCD) and a flame ionization detector (FID). For the TCD channel, the packed column (Carboxen 1000) was used for separating the product gases, which were hydrogen (H_2), oxygen (O_2), carbon monoxide (CO), and carbon dioxide (CO_2). For the FID channel, the capillary column (OV-Plot U) was used for EO and other hydrocarbon product analysis.

For any given Ag loading and support type, the experimental data (with a standard deviation of less than 5%) were averaged and then used to calculate the C_2H_4 and O_2 conversions, the product selectivities, including H_2, CO, CO_2, EO, CH_4, C_2H_6, C_2H_2, and traces of C_3, and the EO yield. These calculations were considered for evaluating the process performance and are defined as follows:

$$\% \text{ Reactant conversion} = \frac{(\text{moles of reactant in} - \text{moles of reactant out}) \times 100}{(\text{moles of reactant in})} \quad (4.1)$$

$$\% \text{ Product selectivity} = \frac{[(\text{number of carbon or hydrogen atom in product})(\text{moles of product produced})] \times 100}{[(\text{number of carbon or hydrogen atom in } C_2H_4) (\text{moles of } C_2H_4 \text{ converted})]} \quad (4.2)$$

$$\% \text{ EO yield} = \frac{(\% \ C_2H_4 \text{ conversion}) \times (\% \text{ EO selectivity})}{100} \quad (4.3)$$

In addition, the power consumption was calculated in a unit of Ws per molecule of converted C_2H_4 or per molecule of produced EO using the following equation:

$$\text{Power consumption} = \frac{P \times 60}{N \times M} \tag{4.4}$$

where P = Power (W)

N = Avogadro's number = 6.02×10^{23} molecules/mol

M = Rate of converted C_2H_4 molecules in feed or rate of produced EO molecules (mol/min).

4.4 Results and Discussion

4.4.1 Catalyst Characterization Results

The specific surface areas of the Al_2O_3- or SiO_2-supported Ag catalysts with various Ag loadings are shown comparatively in Table 4.1. It can be seen that the specific surface area of each loaded support varied slightly with increasing Ag loading, suggesting that the presence of Ag does not significantly affect their specific surface areas, or the specific surface areas of both supports are too low to be significantly affected by Ag loading.

The XRD patterns of the Al_2O_3-supported Ag catalysts are shown in Figure 4.2. For the unloaded support, only α-Al_2O_3 phase was observed. The Ag phase was found at 2θ of 38.2°, when the Ag was loaded on the Al_2O_3 support, and the height of the Ag peak slightly increased with increasing Ag loading from 5 wt.% to 20 wt.%. As also indicated in Table 4.1, the mean Ag crystallite sizes, calculated from the Scherrer equation [27], are in the range of 14.95 nm to 16.61 nm for the Al_2O_3-supported Ag catalysts. On the other hand, for the SiO_2-supported Ag catalysts, there was no clear evidence of any peaks corresponding to SiO_2 (Figure 4.3) because of its amorphous nature [28]. The Ag peak was also found at 2θ of 38.2°, and its intensity increased significantly with increasing Ag loading from 5 wt.% to 20 wt.%. In the cases of 10 wt.% to 20 wt.%, the calculated mean Ag crystallite sizes on the SiO_2 support were also in the range of 14.95 nm to 16.61 nm, similar to the mean Ag crystallite sizes on the Al_2O_3 support (Table 4.1). For the 5 wt.% Ag loading on SiO_2, the mean Ag crystallite size cannot be computed because the Ag particles completely spread as a film-like layer on the SiO_2 surface, as shown later by its SEM image.

Table 4.1 Specific surface areas and mean Ag crystallite sizes of all investigated silver catalysts supported on both Al_2O_3 and SiO_2 particles

Catalyst/Support	Ag loading (wt.%)	Specific surface area (m^2/g)	Mean Ag crystallite size (nm)
Ag/Al$_2$O$_3$	0	1.64	N/A
	5	3.75	14.95
	10	5.13	14.95
	15	3.02	16.61
	20	4.61	16.61
Ag/SiO$_2$	0	0.67	N/A
	5	1.17	N/A
	10	1.17	14.95
	15	1.27	16.61
	20	1.28	16.61
	25	1.31	N/D
	30	1.36	N/D

N/A = Not available, N/D = Not detected
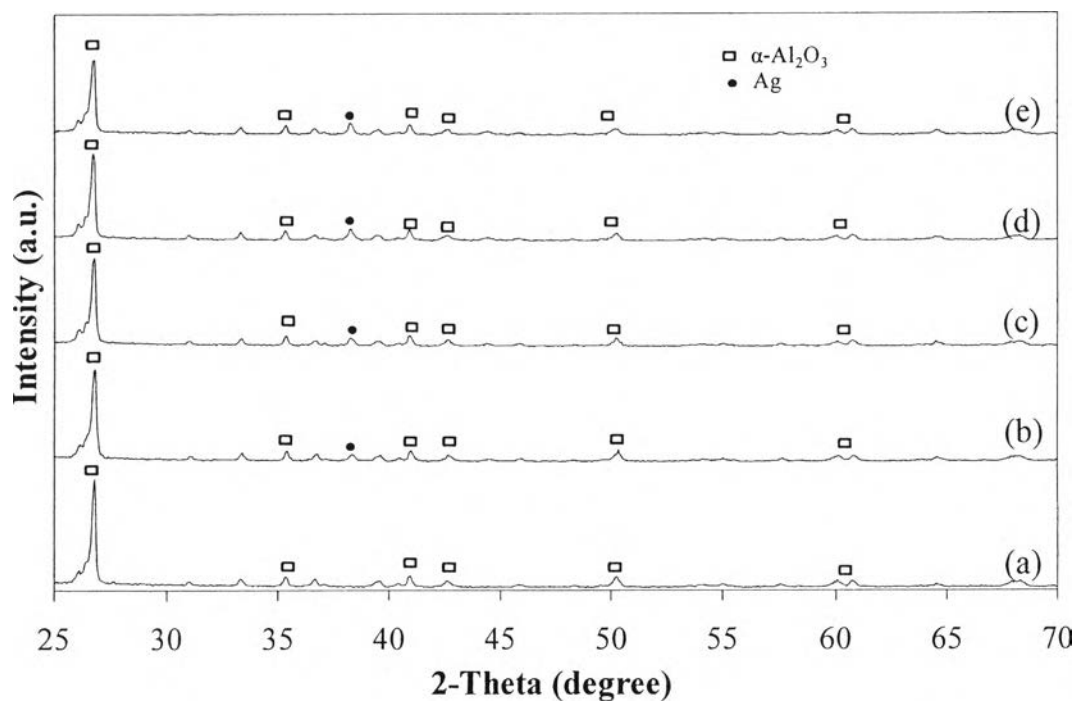
Figure 4.2 XRD patterns of Al_2O_3-supported Ag catalysts: (a) unloaded Al_2O_3 support, (b) 5 wt.% Ag/Al_2O_3, (c) 10 wt.% Ag/Al_2O_3, (d) 15 wt.% Ag/Al_2O_3, and (e) 20 wt.% Ag/Al_2O_3.
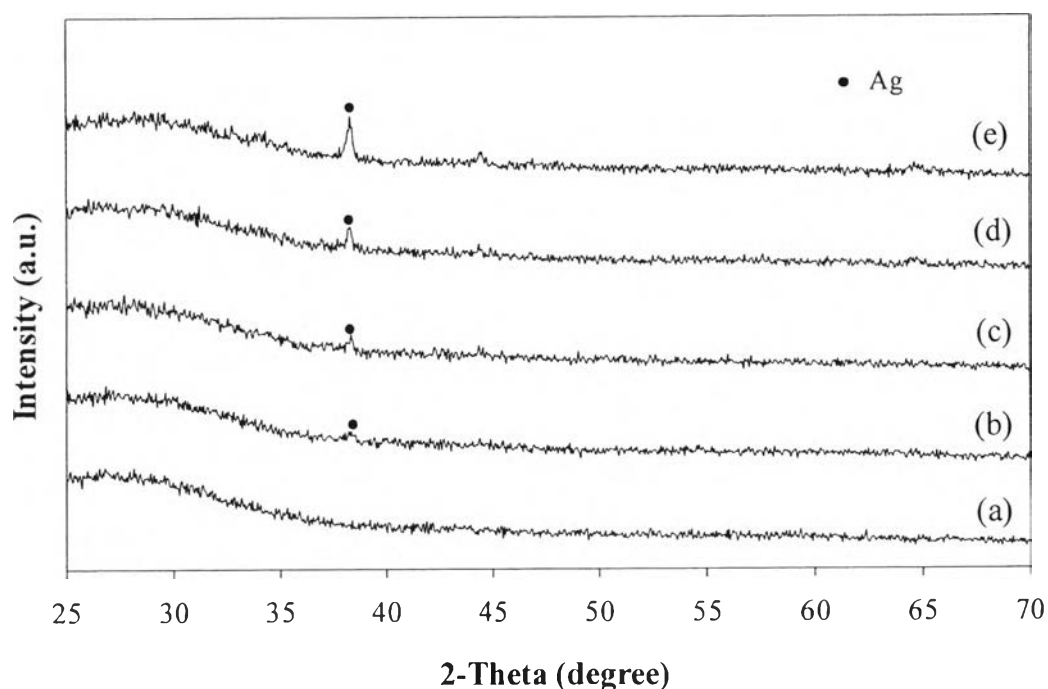
Figure 4.3 XRD patterns of SiO₂-supported Ag catalysts: (a) unloaded SiO₂ support, (b) 5 wt.% Ag/SiO₂, (c) 10 wt.% Ag/SiO₂, (d) 15 wt.% Ag/SiO₂, and (e) 20 wt.% Ag/SiO₂.

The SEM images of the Al₂O₃-supported Ag catalysts with different Ag loadings are shown in Figure 4.4. As shown in Figure 4.4(a), the surface of the unloaded Al₂O₃ support was quite rough. For the 5 wt.% Ag/Al₂O₃ catalyst, Ag particles with various particle sizes were found to well disperse on the Al₂O₃ surface (Figure 4.4(b)). When the Ag loading increased to 10 wt.%, the Ag particles completely covered the Al₂O₃ surface (Figure 4.4(c)). With further increased Ag loading, it was found that some Ag particles grew out from the Al₂O₃ support in a flower-like shape, whereas some Ag particles still had a spherical shape similar to those of the 5 wt.% Ag/Al₂O₃ (Figures 4.4(c) to 4.4(e)). The grown flower-like shape Ag particles, therefore, indicate that the surface area of Al₂O₃ support is not sufficient for Ag particle dispersion. When comparing the SEM images, the Ag loading of 10 wt.% is considered to be an optimum because the Ag particles were not
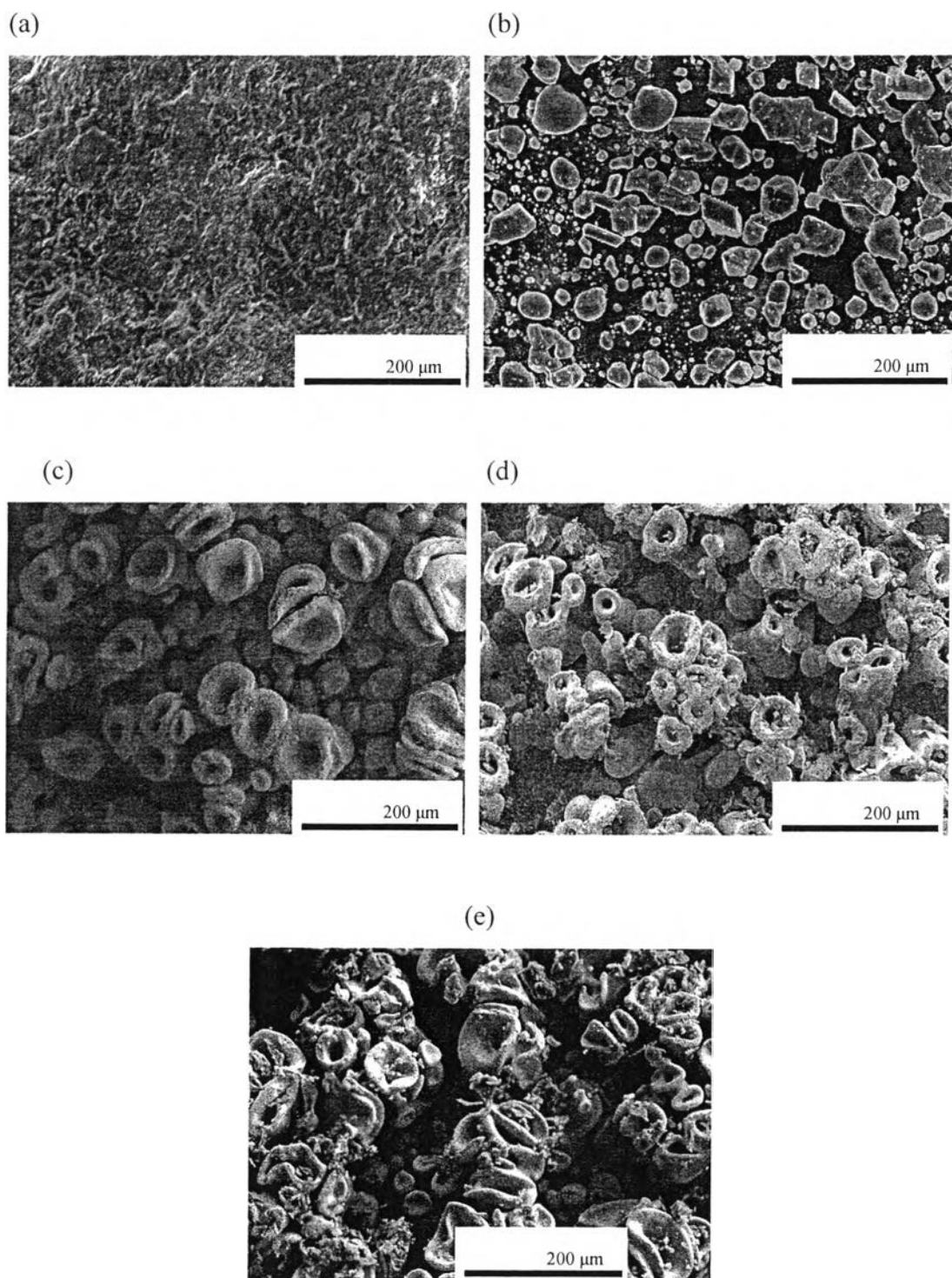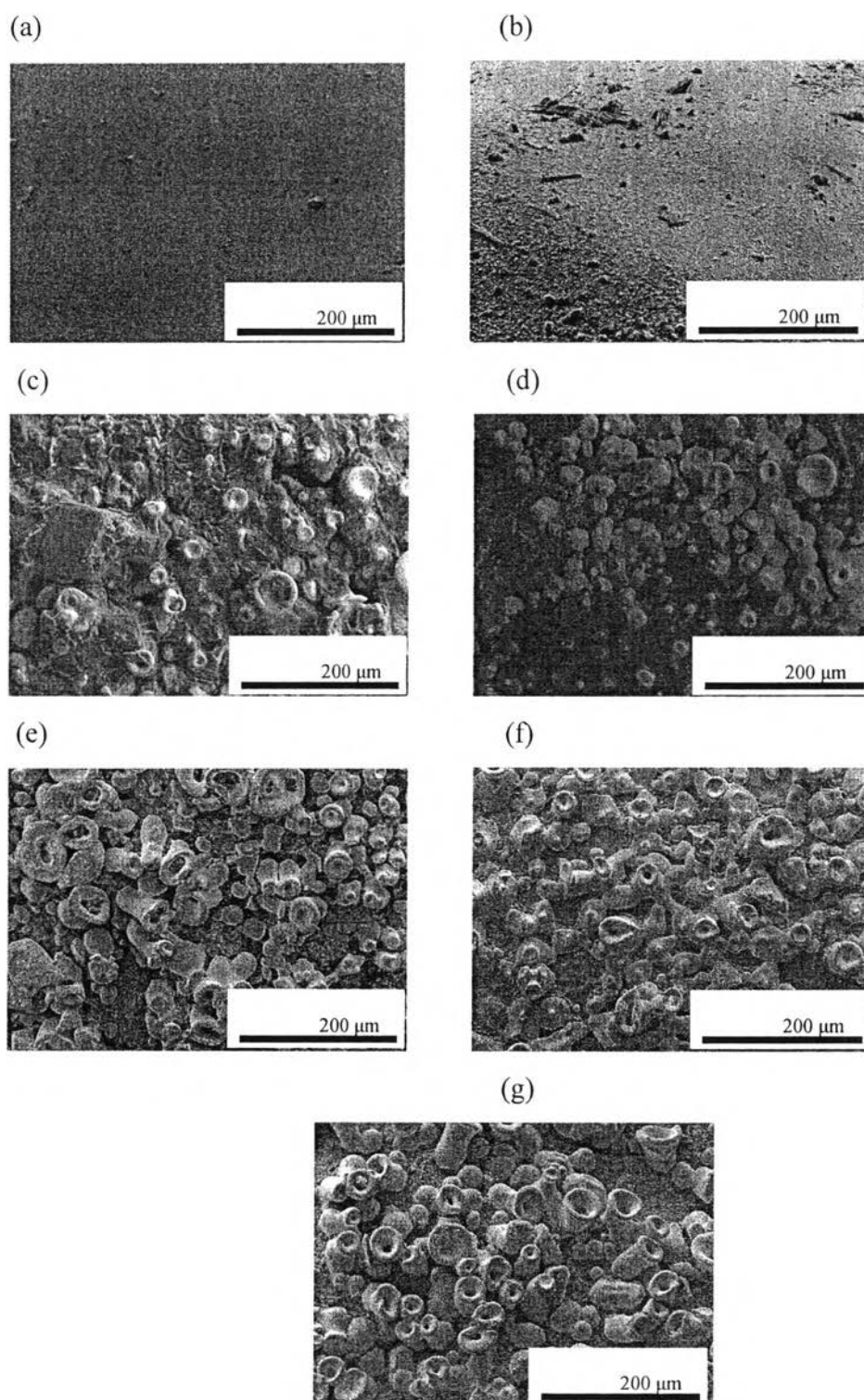
Figure 4.4 SEM images of Al_2O_3-supported Ag catalysts: (a) unloaded Al_2O_3 support, (b) 5 wt.% Ag/Al_2O_3, (c) 10 wt.% Ag/Al_2O_3, (d) 15 wt.% Ag/Al_2O_3, and (e) 20 wt.% Ag/Al_2O_3.

too dense as compared with the 15 wt.% and 20 wt.% Ag loadings, and it was hypothesized to provide the maximum Ag active sites for ethylene epoxidation.

The SEM images of the SiO_2-supported Ag catalysts with different Ag loadings are shown in Figure 4.5. The surface morphology of the unloaded SiO_2 support was quite smooth, as shown in Figure 4.5(a). For the 5 wt.% Ag/SiO_2 catalyst, Ag particles completely covered the SiO_2 surface (as confirmed by the EDX analysis of Ag element), as clearly seen from the rough surface in Figure 4.5(b). With further increasing Ag loading beyond 5 wt.%, the Ag particles grew out from the SiO_2 surface, with spherical and flower-like shapes, similar to the Ag particles on the Al_2O_3 surface (Figures 4.5(c) to 4.5(e)). The number of flower-like Ag particles increased with increasing Ag loading to reach 20 wt.%, which was found to be the highest Ag content that could be loaded on the SiO_2 support since the $AgNO_3$ solution could no longer be prepared due to the limitation of $AgNO_3$ dissolution in distilled water. As mentioned above, the sequential incipient wetness impregnation was used to solve this problem for obtaining the Ag loadings of 25 wt.% and 30 wt.%. For the 25 wt.% Ag/SiO_2 catalyst, the formation of new Ag particles occurred on the old Ag particles around the flower-like ones instead of forming new flower-like ones (Figure 4.5(f)), whereas the 30 wt.% Ag/SiO_2 showed clearly the continuous growth of the flower-like Ag particles (Figure 4.5(g)). The number of the flower-like Ag particles was not observed to increase significantly with increasing Ag loading over 20 wt.%, but the thickness of Ag particles on the SiO_2 surface increased instead. Consequently, the surface area slightly increased. Therefore, the Ag loading of 20 wt.% is considered to be an optimum.

After the ethylene epoxidation reaction experiments, the spent catalysts were analyzed by the TPO technique to determine the coke deposition. The results show that the amounts of coke deposited on the surface of all the spent catalysts were extremely low of only about 0.5 wt.%.

Figure 4.5 SEM images of SiO_2-supported Ag catalysts (a) unloaded silica support, (b) 5 wt.% Ag/SiO_2, (c) 10 wt.% Ag/SiO_2, (d) 15 wt.% Ag/SiO_2, (e) 20 wt.% Ag/SiO_2, (f) 25 wt.% Ag/SiO_2, and (g) 30 wt.% Ag/SiO_2.

4.4.2 Ethylene epoxidation results

As mentioned above, the low-surface-area α-Al_2O_3 is commercially used as the support for Ag catalysts in the epoxidation reaction, because it can provide high EO selectivity [2,29]. Therefore, it was chosen as the first support to investigate the activity of Ag catalysts in the studied DBD plasma system. The effect of plasma volume-to-catalyst weight ratio was initially investigated by using the 5 wt.% Ag/Al_2O_3. The plasma volume-to-catalyst weight ratio was varied from 0.8 cm^3/g to 4 cm^3/g (corresponding to 15 g to 5 g of the catalyst). As shown in Figure 4.6(a), the O_2 conversion tends to increase with increasing plasma volume-to-catalyst weight ratio, while the C_2H_4 conversion under the combined catalytic-DBD system was nearly constant at around 18% and was not much different as compared to that under the sole DBD system. Figure 4.6(b) shows the EO selectivity and yield as a function of plasma volume-to-catalyst weight ratio. From the results, an increase in the plasma volume-to-catalyst weight ratio from 0.8 cm^3/g to 2 cm^3/g increased both the EO selectivity and yield, whereas both the EO selectivity and yield decreased with further increases in the ratio higher than 2 cm^3/g. The results can be explained in that, at the plasma volume-to-catalyst weight ratio lower than 2 cm^3/g (corresponding to the catalyst weight higher than 10 g), the EO selectivity and yield decreased because adding too much catalyst can considerably interfere with plasma discharges by decreasing the stability and uniformity of the plasma, even though the Ag active sites increased with increased catalyst weight. In contrast, at the plasma volume-to-catalyst weight ratio higher than 2 cm^3/g (corresponding to the catalyst weight lower than 10 g), although plasma discharges were observed to be more uniform and stable with decreasing catalyst weight, the Ag active sites on the Al_2O_3 support accordingly decreases, resulting in lowering the ethylene epoxidation activity. These results imply that the amount of the catalyst used in the combined catalytic-DBD system has a significant influence on the ethylene epoxidation activity, and so it needs to be optimized. Therefore, it can be concluded that the plasma volume-to-catalyst weight ratio of 2 cm^3/g was the optimum value for the combined catalytic-DBD system in this present work, exhibiting the highest ethylene epoxidation activity, possibly due to the maximum synergistic effect between the catalyst and plasma discharges at this ratio. Interestingly, the plasma volume-to-

(a)

(b)

(c)

(d)
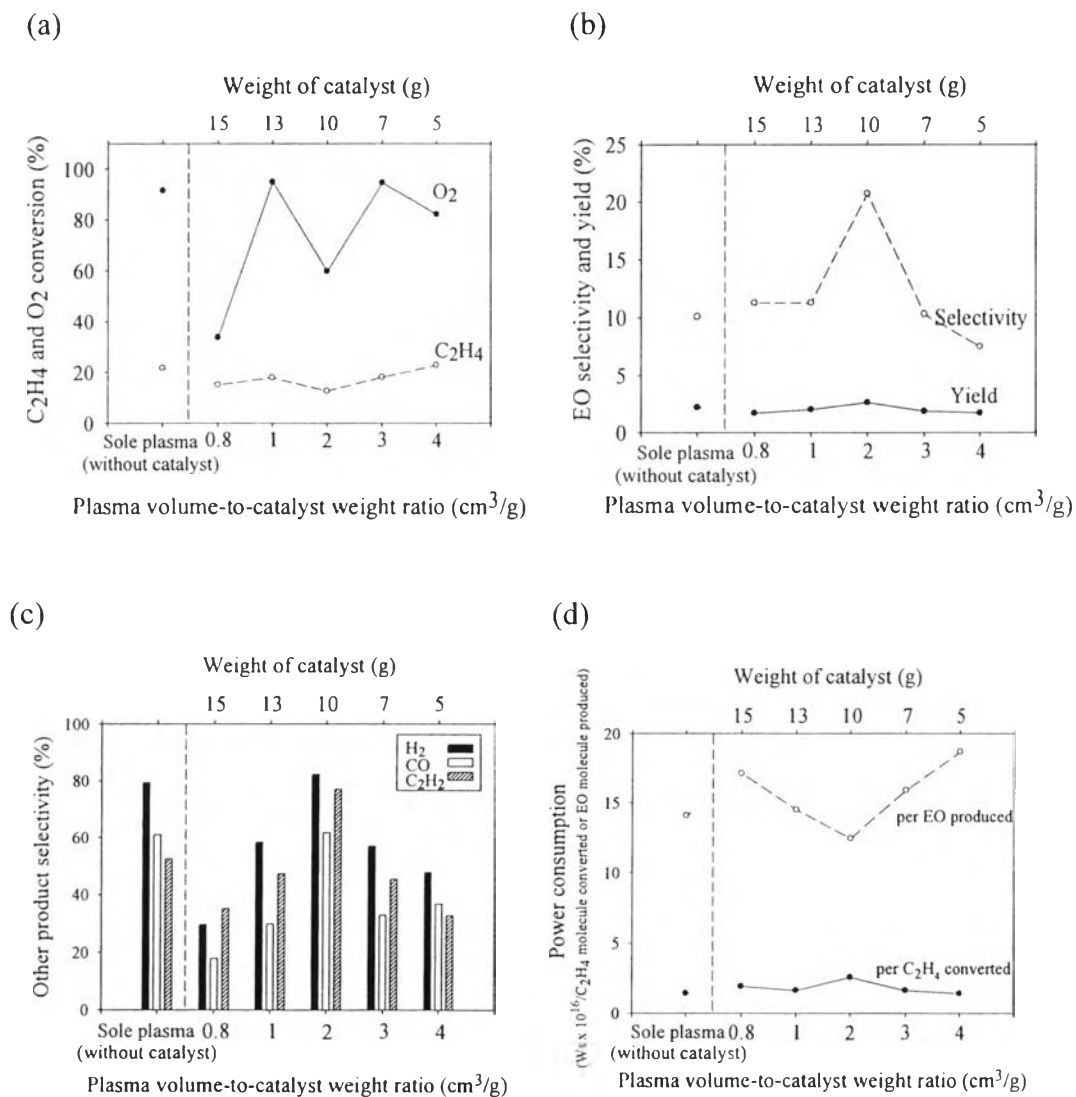
Figure 4.6 (a) C_2H_4 and O_2 conversions, (b) EO selectivity and yield, (c) other product selectivities, and (d) power consumptions as a function of plasma volume-to-catalyst weight ratio of 5 wt.% Ag/Al_2O_3 (an O_2/C_2H_4 feed molar ratio of 1/4, a total feed flow rate of 50 cm^3/min, an electrode gap distance of 0.7 cm, an input frequency of 500 Hz, and an applied voltage of 19 kV).

catalyst weight ratio much more significantly affected the EO selectivity than the EO yield. Hence, the EO selectivity should be used as a prime parameter in determining the process performance of this ethylene epoxidation reaction. Moreover, the combined catalytic-DBD system with 2 cm^3/g of the plasma volume-to-catalyst

weight ratio provided much higher EO selectivity while EO yield was slightly increased as compared to the sole DBD system. This finding indicates that the presence of supported Ag catalysts in the DBD system can enhance the ethylene epoxidation performance in the terms of EO selectivity and yield.

The selectivities for other main products, i.e. H_2, CO, and C_2H_2, as a function of plasma volume-to-catalyst weight ratio are shown in Figure 4.6(c), whereas those for other by-products, i.e. CO_2, CH_4, C_2H_6, C_2H_2, and C_3H_8, are not shown due to their extremely low concentrations (lower than 5%). The results show that the selectivities for H_2, CO, and C_2H_2 had the same trends as the EO selectivity. The increase in plasma volume-to-catalyst weight ratio from 0.8 cm^3/g to 2 cm^3/g increased the selectivities for all other main products, but they decreased with further increasing plasma volume-to-catalyst weight ratio higher than 2 cm^3/g. These results imply that the Ag active sites on the Al_2O_3 support not only catalyze the ethylene epoxidation, but also affect the other side and subsequent reactions during the plasma process. Comparing the combined catalytic-DBD system with the sole DBD plasma, it can be seen that the selectivities for H_2 and CO under both systems are not that different, whereas the selectivity for C_2H_2 under the sole DBD system was lower as compared to the combined catalytic-DBD system at the plasma volume-to-catalyst weight ratio of 2 cm^3/g.

In contrast to the product selectivity results, the power consumption per molecule of EO produced decreased with increasing plasma volume-to-catalyst weight ratio to reach a minimum value at the plasma volume-to-catalyst weight ratio of 2 cm^3/g, after which it adversely increased with further increasing plasma volume-to-catalyst weight ratio (Figure 4.6(d)). However, the power consumption per molecule of C_2H_4 converted remained almost unchanged with respect to the plasma volume-to-catalyst weight ratio. The power consumption per molecule of EO was about one order of magnitude higher than that per molecule of C_2H_4 converted. Therefore, the power consumption per molecule of EO produced should also be considered to be another prime parameter in determining the process performance, in addition to the EO selectivity. From the overall results, the plasma volume-to-catalyst weight ratio of 2 cm^3/g was the optimum value, which was used for further investigation of the effect of Ag loading, because it provided not only the highest EO

selectivity and the lowest power consumption per molecule of EO produced in the case of the combined catalytic-DBD system, but also higher EO selectivity at a level of more than two-fold compared to the sole DBD system.

The effect of Ag loading was investigated by varying Ag loading from 5 wt.% to 20 wt.% on the Al_2O_3 support and 5 wt.% to 30 wt.% on the SiO_2 support. From the results shown in Figure 4.7(a), the C_2H_4 and O_2 conversions tend to decrease with increasing Ag loading on the Al_2O_3 support. The EO selectivity was significantly affected by Ag loading, as shown in Figure 4.7(b). With increasing Ag loading up to 10 wt.%, the EO selectivity sharply increased, but it tended to decrease when the Ag loading further increased above 10 wt.%. The results show that the Ag loading of 10 wt.% provided the highest EO selectivity. However, the EO yield was not significantly changed with increasing Ag loading because, when the EO selectivity increased, the C_2H_4 conversion adversely decreased. This led to a possible trade-off effect on the EO yield.

The selectivities for other main products, i.e., H_2, CO, and C_2H_2, as a function of Ag loading are shown in Figure 4.7(c). From the results, the pure Al_2O_3 support provided very low selectivities for CO and C_2H_2, but gave the highest selectivity for H_2, as compared to the sole plasma and the plasma with all Al_2O_3-supported Ag catalysts. The selectivities for H_2 and C_2H_2 insignificantly changed when increasing Ag loading from 5 wt.% to 20 wt.%, while the selectivity for CO tended to increase with increasing Ag loading from 0 wt.% to 10 wt.%, and then decreased with further increasing Ag loading higher than 10 wt.%. From the results, the pure Al_2O_3 support was found to be a good catalyst for producing H_2 while the 10 wt.% Ag-loaded Al_2O_3 catalyst gave the highest EO selectivity.

Figure 4.7(d) shows the power consumptions per C_2H_4 molecule converted and per EO molecule produced as a function of Ag loading. The results indicate that the presence of the Ag catalyst loaded on the Al_2O_3 support could affect the power consumptions. From the results, the power consumption per molecule of C_2H_4 converted gradually increased with increasing Ag loading, whereas the power consumption per molecule of EO initially decreased when the Ag loading increased to 5 wt.%, but tended to slightly increase with further increases in Ag loading over 5 wt.%. Comparing various Ag loadings (Figures 4.7), the Ag loading of 10 wt.% is

(a)

(b)

(c)

(d)
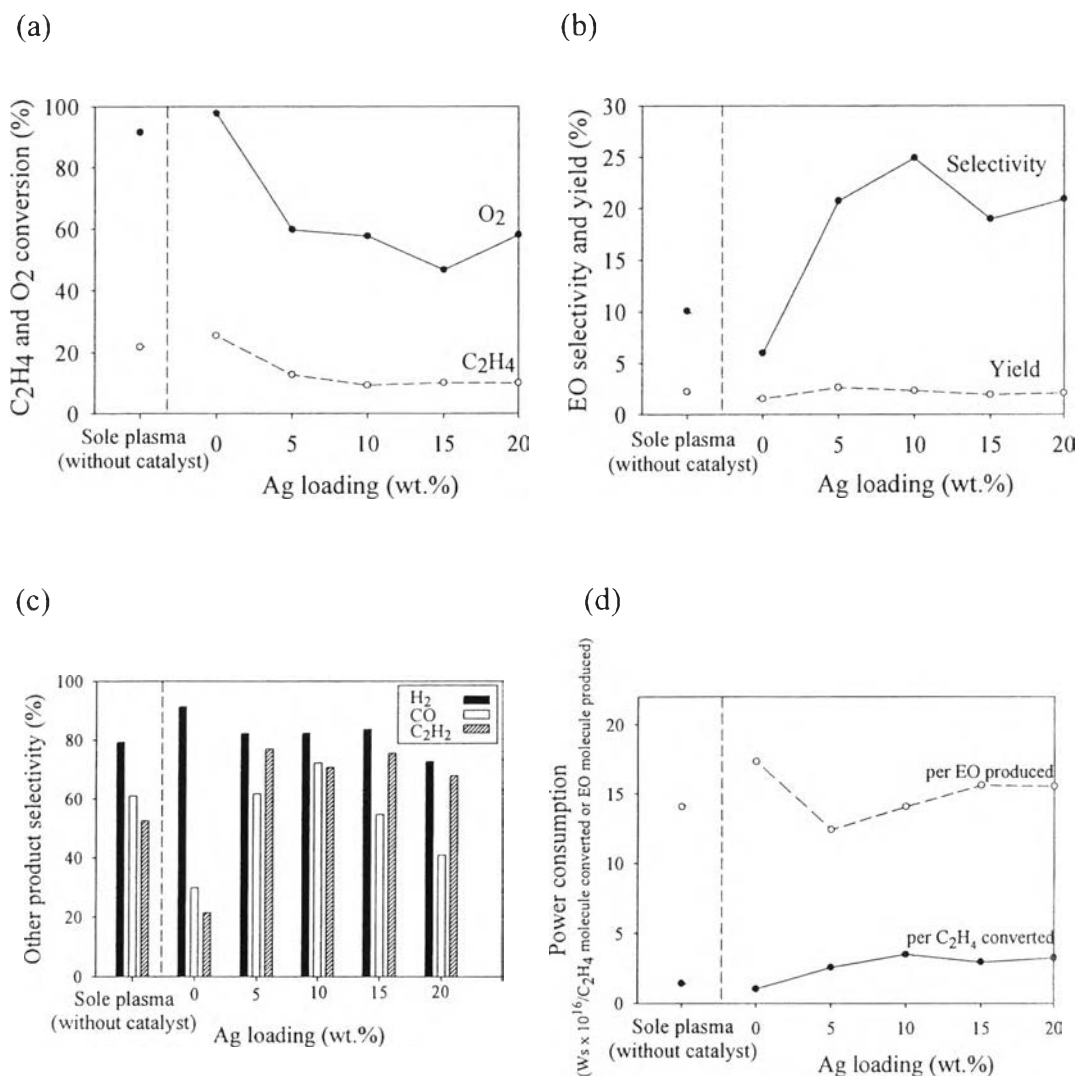
Figure 4.7 (a) C_2H_4 and O_2 conversions, (b) EO selectivity and yield, (c) other product selectivities, and (d) power consumptions as a function of Ag loading on Al_2O_3 support in the DBD plasma reactor (a plasma volume-to-catalyst weight ratio of 2 cm^3/g (10 g of catalyst), an O_2/C_2H_4 feed molar ratio of 1/4, a total feed flow rate of 50 cm^3/min, an electrode gap distance of 0.7 cm, an input frequency of 500 Hz, and an applied voltage of 19 kV).

considered to be the optimum Ag loading on the Al_2O_3 particles because it provided the highest epoxidation activity in the terms of EO selectivity with relatively high EO yield and comparatively low power consumption per molecule of EO produced. These results agree well with the SEM images (Figure 4.4) that the Ag particles of

the 10 wt.% Ag loading were not too compact on the Al_2O_3 surface and seemed to have sufficient Ag active sites to catalyze the ethylene epoxidation.

To comparatively investigate the effect of SiO_2 support for the Ag catalysts on the epoxidation activity, the plasma volume-to-catalyst weight ratio of 2 cm^3/g was also used. Figures 4.8 shows the C_2H_4 and O_2 conversions, the EO selectivity and yield, the other product selectivities, and the power consumptions as a function of Ag loading on the SiO_2 support. As shown in Figure 4.8(a), the C_2H_4 conversion slightly increased with increasing Ag loading from 0 wt.% to 5 wt.% and then tended to decrease with further increases in Ag loading, whereas the O_2 conversion reached a maximum of 98% at the Ag loading of 5 wt.% and then suddenly decreased with increasing Ag loading beyond 10 wt.%. From the results shown in Figure 4.8(b), the EO selectivity tended to remain almost unchanged in the Ag loading range of 0 wt.% to 15 wt.% and suddenly increased to reach a maximum at Ag loading of 20 wt.%, which is three times higher as compared to the sole DBD system. However, the EO selectivity decreased substantially with further increases in Ag loading over 20 wt.%.

Figure 4.8(c) shows the selectivities for the other main products, i.e., H_2, CO, and C_2H_2. From the results, all Ag catalysts on the SiO_2 support provided lower other main product selectivities as compared to the unloaded SiO_2 support, except the C_2H_2 selectivity at the highest Ag loading of 30 wt.%. This indicates that the Ag active sites on the SiO_2 support seem to promote the ethylene epoxidation and reduce the further reactions of EO to other products. Moreover, the selectivities for H_2, CO, and C_2H_2 tended to increase with increasing Ag loading, suggesting that an increase in Ag loading on the SiO_2 support can promote both the ethylene epoxidation and other reactions. Hence, there must be an optimum Ag loading for the ethylene epoxidation reaction.

The power consumption per molecule of C_2H_4 converted slightly changed with increasing Ag loading, whereas the power consumption per molecule of EO produced decreased with increasing Ag loading from 0 wt.% to 10 wt.%, and then tended to fluctuate slightly in a narrow range with further increases in Ag loading higher than 10 wt.% (Figure 4.8(d)). Comparing Ag loadings, the 20 wt.% Ag-loaded SiO_2 catalyst was found to be the best catalyst for the ethylene

epoxidation reaction because it yielded the highest EO selectivity with comparatively low power consumption per molecule of EO produced. These results concur with the SEM images (Figure 4.5) that the number of Ag particles of 20 wt.% Ag loading was found to reach a maximum.

(a)   (b)

(c)   (d)
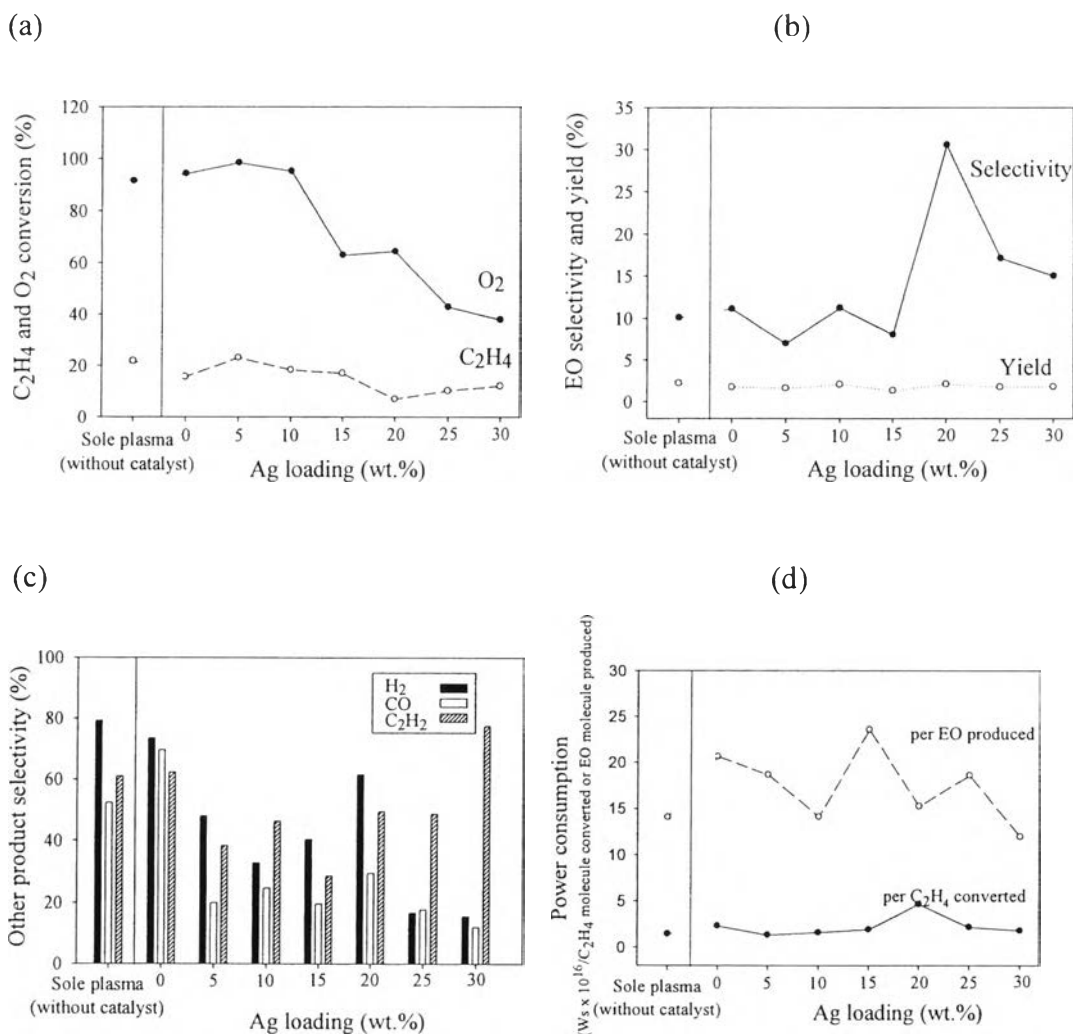
Figure 4.8 (a) C_2H_4 and O_2 conversions, (b) EO selectivity and yield, (c) other product selectivities, and (d) power consumptions as a function of Ag loading on SiO_2 support in the DBD plasma reactor (a plasma volume-to-catalyst weight ratio of 2 cm^3/g (10 g of catalyst), an O_2/C_2H_4 feed molar ratio of 1/4, a total feed flow rate of 50 cm^3/min, an electrode gap distance of 0.7 cm, an input frequency of 500 Hz, and an applied voltage of 19 kV).

The ethylene epoxidation performances under the DBD system with both supported Ag catalysts at the optimum loadings were compared to those of the sole DBD system and the DBD system with the unloaded supports. As shown in Figure 4.9(a), the O_2 conversions of the DBD system with each unloaded support were comparable to that of the sole DBD system; however, the O_2 conversion decreased substantially when the Ag catalysts on both supports were applied to the DBD system under their own optimum loadings. The C_2H_4 conversion had quite the same trend as the O_2 conversion; that is, the C_2H_4 and O_2 conversions of the DBD system with either support were much lower than those of the sole plasma system and the plasma systems with each unloaded support. This is possibly because the Ag loading on the supports significantly alters the plasma behaviors as compared to the unloaded supports. Further investigation is required with the emphasis on the physicochemical and electrical properties of Ag particles under the studied conditions.

Figure 4.9(b) shows the effects of support type and Ag loading on the EO selectivity and yield. From the results, the unloaded SiO_2 support showed a slightly higher EO selectivity with a slightly lower EO yield while the plasma system with the unloaded Al_2O_3 support provided both lower EO selectivity and yield as compared to the sole plasma system. Interestingly, the presence of both Ag catalysts loaded on the Al_2O_3 and SiO_2 supports gave the significant increase only in the EO selectivities, but not for the EO yields. In a comparison between these two studied supports, the SiO_2 support exhibited a higher EO selectivity than the Al_2O_3 support. The results can be explained in that the SiO_2 support had a lower electrical resistivity than the Al_2O_3 support [30], leading to altering the plasma discharge behaviors. In addition, the DBD system applied with the SiO_2 support was found to provide better stability and uniformity of the plasma than that with the Al_2O_3 support. As mentioned above, the EO selectivity and yield under the DBD system with the unloaded SiO_2 support were not much different from those of the sole plasma system. The EO selectivity, however, was significantly enhanced when the DBD system was operated in the presence of Ag catalysts. The explanation is that the extremely high electrical conductivity of the Ag particles can overcome the plasma discharge interference by the low-electrical conductivity of both supports. The
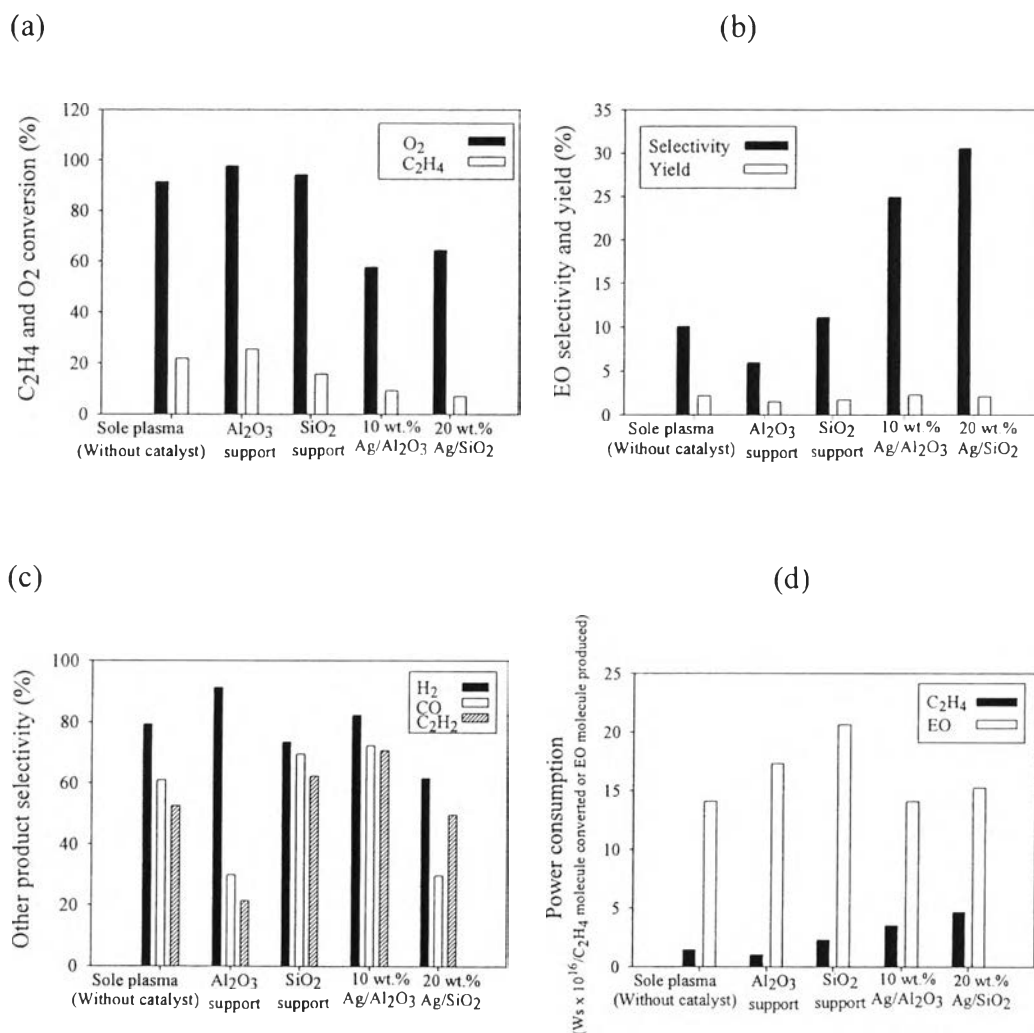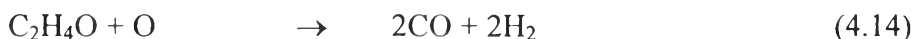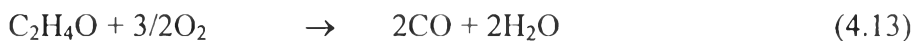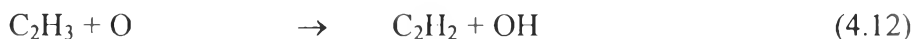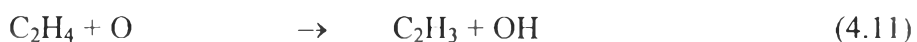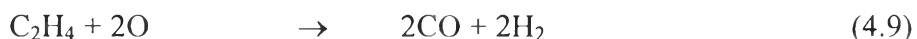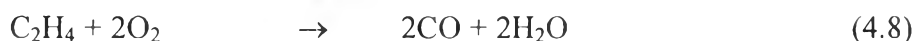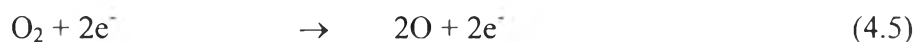
Figure 4.9 (a) C_2H_4 and O_2 conversions, (b) EO selectivity and yield, (c) other product selectivities, and (d) power consumptions of the DBD plasma reactor with Ag catalysts loaded on two supports (Al_2O_3 and SiO_2) as compared to the sole DBD plasma reactor (a plasma volume-to-catalyst weight ratio of 2 cm^3/g (10 g of catalyst), an O_2/C_2H_4 feed molar ratio of 1/4, a total feed flow rate of 50 cm^3/min, an electrode gap distance of 0.7 cm, an input frequency of 500 Hz, and an applied voltage of 19 kV).
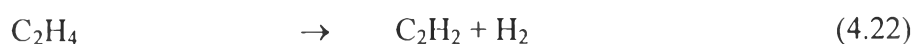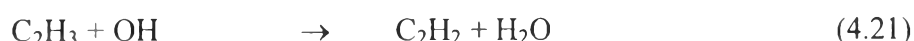
plasma discharge, generated by the DBD system with both supported silver catalysts, was found to exhibit higher stability and uniformity as compared to those with both unloaded supports. The results suggest that the Ag active sites are responsible for the enhancement of the ethylene epoxidation reaction in the DBD environment.

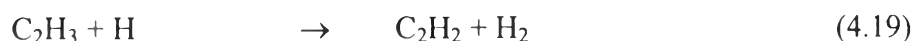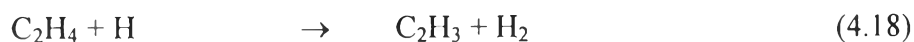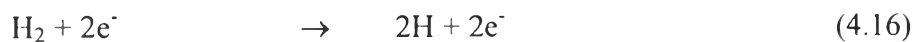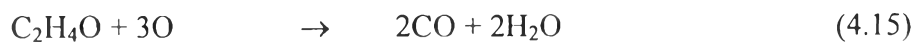Comparing the two supports, the SiO_2 support (with an optimum Ag loading of 20 wt.%) provided a higher EO selectivity than the Al_2O_3 support (with an optimum Ag loading of 10 wt.%). These results can possibly be explained by the fact that the SiO_2 support generally possesses a lower acidity as compared to the Al_2O_3 support, as also reported by Volckmar et al. [31]. Since a catalyst support surface with a lower acidity favors the ethylene epoxidation as compared to other undesired secondary surface reactions [9], hence, the SiO_2 support can be considered to be a more suitable support for Ag catalysts for the ethylene epoxidation in the investigated combined catalytic-DBD plasma system. In addition, the SiO_2 support has lower electrical resistivity than the Al_2O_3 support, leading to more stable and uniform plasma discharges, as mentioned above. However, it was found that the EO yield remained almost unchanged in the range of 1.5-2.3% for all cases (Figure 4.9(b)).

Figure 4.9(c) shows the selectivities for other main products, i.e., H_2, CO, and C_2H_2. Interestingly, it was observed that, among all studied systems, the 20 wt.% Ag/SiO_2 catalyst provided the lowest selectivities for H_2 and CO, as well as a comparatively low selectivity for C_2H_2. Therefore, the 20 wt.% Ag/SiO_2 can be considered to be a promising catalyst to be used in the combined catalytic-DBD plasma system for EO production. The power consumptions of all studied systems are shown in Figure 4.9(d). From the detected main products, all possible reactions that may predominantly occur in the DBD plasma system can be proposed as follows:

$$O_2 + 2e^- \rightarrow 2O + 2e^- \tag{4.5}$$

$$C_2H_4 + 1/2O_2 \rightarrow C_2H_4O \tag{4.6}$$

$$C_2H_4 + O \rightarrow C_2H_4O \tag{4.7}$$

$$C_2H_4 + 2O_2 \rightarrow 2CO + 2H_2O \tag{4.8}$$

$$C_2H_4 + 2O \rightarrow 2CO + 2H_2 \tag{4.9}$$

$$C_2H_4 + 4O \rightarrow 2CO + 2H_2O \tag{4.10}$$

$$C_2H_4 + O \rightarrow C_2H_3 + OH \tag{4.11}$$

$$C_2H_3 + O \rightarrow C_2H_2 + OH \tag{4.12}$$

$$C_2H_4O + 3/2O_2 \rightarrow 2CO + 2H_2O \tag{4.13}$$

$$C_2H_4O + O \rightarrow 2CO + 2H_2 \tag{4.14}$$

$$C_2H_4O + 3O \rightarrow 2CO + 2H_2O \tag{4.15}$$

$$H_2 + 2e^- \rightarrow 2H + 2e^- \tag{4.16}$$

$$H_2O + 2e^- \rightarrow H + OH + 2e^- \tag{4.17}$$

$$C_2H_4 + H \rightarrow C_2H_3 + H_2 \tag{4.18}$$

$$C_2H_3 + H \rightarrow C_2H_2 + H_2 \tag{4.19}$$

$$C_2H_4 + OH \rightarrow C_2H_3 + H_2O \tag{4.20}$$

$$C_2H_3 + OH \rightarrow C_2H_2 + H_2O \tag{4.21}$$

$$C_2H_4 \rightarrow C_2H_2 + H_2 \tag{4.22}$$
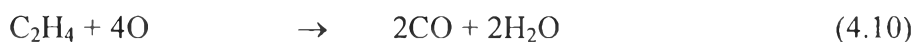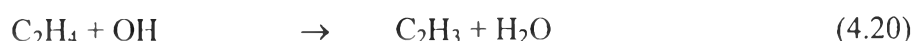
When comparing the combined catalytic-DBD system with the sole DBD system, the supported Ag catalysts, especially the 20 wt% Ag/SiO_2 catalyst, promoted the ethylene epoxidation (4.6,4.7) due to the observed higher EO selectivity, and tended to suppress the combustion (4.8–4.10, 4.13–4.15) and dehydrogenation (4.11, 4.12, 4.18–4.22) reactions due to the lower selectivities for H_2, CO, and C_2H_2, whereas the combustion and dehydrogenation reactions could favorably occur in the sole DBD system, leading to decreasing EO selectivity and increasing selectivities for other main products.

The power consumption per molecule of C_2H_4 converted was found to be higher for the plasma system with the Ag catalysts on both studied supports than those of the sole plasma systems with and without both unloaded supports. Interestingly, the power consumption per molecule of EO produced of the DBD system decreased when it was applied with the Ag catalysts loaded on both supports. Overall, the SiO_2 support with an optimum Ag loading of 20 wt.% was considered to be a highly potential catalyst for the combined catalytic-DBD plasma system for the ethylene epoxidation because it provided the highest EO selectivity (almost three times higher as compared to the sole DBD system) with the lowest H_2 and CO selectivities, as well as a comparatively low C_2H_2 selectivity and low power consumption per molecule of EO produced.

4.5 Conclusions

The epoxidation reaction of ethylene was investigated using a DBD system in the absence and presence of both the Al_2O_3- and SiO_2-supported Ag catalysts. The presence of Ag catalysts was found to enhance EO selectivity. Moreover, the Ag catalysts on the SiO_2 particles were experimentally found to be more effective than those on the Al_2O_3 particles in catalyzing the ethylene epoxidation in terms of EO selectivity. The optimum Ag loading on the SiO_2 particles was found to be 20 wt.%, at which the maximum EO selectivity and the minimum H_2 and CO selectivities were obtained at the operating applied voltage and input frequency of 19 kV and 500 Hz, respectively. Under these optimum conditions, the power consumption was found to be 15.26×10^{-16} Ws per molecule of EO produced.

4.6 Acknowledgements

4.7 References

1. Lefort TE, Fr. Patent 729 (1931) 952.

2. http://en.wikipedia.org/wiki/Ethylene_oxide (accessed on November 4, 2010)

3. http://www.labsafety.com/refinfo/ezfacts/ezf176.htm (accessed on November 4, 2010)

4. Campbell CT, Paffett MT (1984) Appl Surf Sci 19:28

5. Campbell CT, Koel BE (1985) J Catal 92:272

6. Tan SA, Grant RB, Lambert RM (1986) J Catal 100:383

7. Tories N, Verikios XE (1987) J Catal 108:161

8. Jun Y, Jingfa D, Xiaohong Y, Shi Z (1992) Appl Catal A: Gen 92:73

9. Mao CF, Vannice MA (1995) Appl Catal A 122:61

10. Jankowick JT, Barteau MA (2005) J Catal 236:379

11. Dellamorte JC, Lauterback J, Barteau MA (2007) Catal Today 120:182

12. Rojluechi S, Chavadej S, Schwank JW, Meeyoo V (2007) Catal Commun 1:57

13. Marta CN, de Carvalho A, Passos FB, Schmal M (2007) J Catal 248:124

14. Chavadej S, Tansuwan A, Sreethawong T (2008) Plasma Chem Plasma Process 28:643

15. Sreethawong T, Suwannabart T, Chavadej S (2009) Chem Eng J 115:396

16. Seyedmonir SR, Plishchke JK, Vannic MA, Young MW (1990) J Catal 123:534

17. Bradford MCJ, Fuentes DX (2002) Catal Commun 3:51

18. Rojluechai S, Chavadej S, Schwank JW, Meeyoo V (2006) J Chem Eng Jpn 39:321

19. Lee JK, Verykbs XE, Pitchai R (1989) Appl Catal 50:171

20. Yong YS, Kennedy EM, Cant NM (1991) Appl Catal 76:31

21. Rosacha LA, Anderson GK, Bechtold LA, Coogan JJ, Heck HG, Kang M, McCulla WH, Tennant RA, Wantuck PJ, NATO ASI series (1993) 34, part B.

22. Suhr H, Schmid H, Pfeundschuh H, Lacocca D (1984) Plasma Chem Plasma Process 4:285

23. Heintze M, Pietruszka B (2004) Catal Today 87:21

24. Sreethawong T, Suwannabart T, Chavadej S (2008) Plasma Chem Plasma Process 28:629

25. Chavadej S, Kiattubolpaiboon W, Rangsunvigit P, Sreethawong T (2007) J Mol Catal A: Chem 263:128

26. Sreethawong T, Permsin N, Suttikul T, Chavadej S (2010) Plasma Chem Plasma Process 30:503

27. Cullity BD (1978) Element of X-ray Diffraction, Addison-Wesley Publication Company, Massachusetts.

28. Apostolos PF, Kostas ST (2007) Catal Today 127:148

29. Oyama ST (2008) Mechanisms in Homogeneous and Heterogeneous Epoxidation Catalysis, Elsevier Publication Company, Oxford.

30. http://accuratus.com/alumax.html (accessed on November 4, 2010)

31. Volckmar CE, Bron M, Bentrup U, Martin A, Claus P (2009) J Catal 261:1